



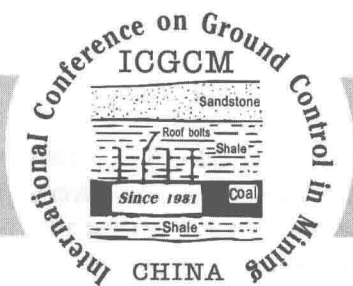
# 煤矿岩层控制 理论与技术进展

——37届国际采矿岩层控制会议（中国·2018）论文集

主 编 张 农, [美]彭赐灯 (Syd S. Peng)

副主编 李桂臣 吴锋锋 程敬义

中国矿业大学出版社



# 煤矿岩层控制 理论与技术进展

——37届国际采矿岩层控制会议（中国·2018）论文集

主 编 张 农 [美]彭赐灯 (Syd S.Peng)

副主编 李桂臣 吴锋锋 程敬义

中国矿业大学出版社

## 内 容 简 介

本书收录了国内外煤矿开采岩层控制领域的学术论文 31 篇,集中展示了国际采矿岩层控制领域近年来的理论与技术创新成果。主要包括采场岩层控制理论与技术、坚硬顶板岩层控制理论与技术、巷道围岩控制与防治技术、深部岩石力学与工程应用、大倾角煤层开采矿压控制理论与技术、煤层群协调开采矿压控制理论与技术、煤与瓦斯共采理论与技术、充填开采理论与技术、智能岩层控制、矿山灾害防治等与采矿岩层控制相关的主题等。

本书可供从事煤矿开采方面科研、设计、工程技术及管理人员阅读参考,也可供高等院校矿业工程研究领域师生参考。

### 图书在版编目(CIP)数据

煤矿岩层控制理论与技术进展:37 届国际采矿岩层控制会议(中国·2018)论文集/张农,(美)彭赐灯(Syd S. Peng)

主编. —徐州:中国矿业大学出版社,2018.9

ISBN 978 - 7 - 5646 - 4126 - 9

I. ①煤… II. ①张… ②彭… III. ①煤矿开采—岩层控制—文集 IV. ①TD325—53

中国版本图书馆 CIP 数据核字(2018)第 223004 号

书 名 煤矿岩层控制理论与技术进展

——37 届国际采矿岩层控制会议(中国·2018)论文集

主 编 张 农 [美]彭赐灯(Syd S. Peng)

责任编辑 王美柱

责任校对 仓小金

出版发行 中国矿业大学出版社有限责任公司

(江苏省徐州市解放南路 邮编 221008)

营销热线 (0516)83885307 83884995

出版服务 (0516)83885767 83884920

网 址 <http://www.cumtp.com> E-mail: cumtpvip@cumtp.com

印 刷 江苏淮阴新华印刷厂

开 本 787×1092 1/16 印张 27.25 字数 751 千字

版次/印次 2018 年 9 月第 1 版 2018 年 9 月第 1 次印刷

定 价 158.00 元

(图书出现印装质量问题,本社负责调换)

# 大会学术委员会

主 席：

Syd S. Peng 钱鸣高 彭苏萍 袁 亮 何满潮 康红普 顾大钊  
刘 波 葛世荣 刘 峰 祁和刚

副主席（以姓氏笔画为序）：

于 斌 才庆祥 王家臣 卞正富 叶继红 冯夏庭 冯 涛 刘泉声  
齐庆新 池秀文 许升阳 李夕兵 李树刚 杨仁树 吴爱祥 张东升  
张 农 周 英 孟祥瑞 郝传波 姜德义 梁卫国 梁 冰 靖洪文  
窦林名 谭云亮

委 员（以姓氏笔画为序）：

丁建丽 万志军 马占国 王卫军 冯国瑞 伍永平 华心祝 刘长友  
许兴亮 纪洪广 李兴华 杨永辰 杨圣奇 张吉雄 张宏伟 张国华  
尚 涛 柏建彪 骆振福 郭文兵 黄炳香 曹胜根 屠世浩

# 大会组织委员会

主 任:张 农 靖洪文

副主任:李兴华 马占国 张吉雄 万志军 杨圣奇 王晓琳 浦 海  
范 军 李 亭 李桂臣 Brijes Mishra

成 员:牟宗龙 黄炳香 王旭锋 方新秋 王襄禹 杨 真 姚强岭  
周 伟 马文顶 曹安业 黄艳利 范钢伟 徐 营

秘书长:李桂臣

秘 书:吴锋锋 程敬义 杨 真 李 剑 闫 帅 王 君 吴元周  
殷 实

## 前 言

国际采矿岩层控制会议(International Conference on Ground Control in Mining,简称 ICGCM)自 1981 年起在美国举办,至今已成功举办 36 届。我国煤炭开采技术飞速发展,为了便于我国学者与国际采矿岩层控制领域的学者进行广泛交流,提高我国在采矿岩层控制领域的研究与应用水平,提升我国在国际采矿行业的国际影响力,经与 ICGCM 组委会协商,将定期在中国举办“国际采矿岩层控制会议(中国)”。

此次国际会议是第五次在中国召开,总第 37 届。会议的目标是创建一个在煤炭开采岩层控制方面技术分享与讨论的平台。会议主席团由国内外采矿岩层控制领域权威专家组成,包括中国工程院院士和美国工程院院士。会议的交流内容不仅注重采矿岩层控制的基础理论,而且也重视煤炭开采方面的实际问题与前沿技术,将为世界采矿技术的发展起到重要的理论和实际指导意义。

会议从 2018 年 2 月开始征集论文至 2018 年 9 月,共收到来自国内外煤矿开采岩层控制领域的中文、英文论文 41 篇,通过大会学术委员会筛选,收录 31 篇论文。

会议组委会李桂臣、牟宗龙、王襄禹、吴锋锋、程敬义等在会议的论文征集与出版等方面做了大量工作。Syd S. Peng 院士给出了许多建设性建议和指导,为此次会议的顺利举办和提升会议的国际性作出了重要贡献。

组委会  
2018 年 9 月

# 目 录

Detection of floor water inrush risks for deep longwall mining in a Chinese coal mine .....	HE Dongsheng, ZHANG Yang, WANG Fangtian(1)
动压影响煤柱下方沿空巷道微震特征及破坏机制 .....	李术才,王雷,江贝,等(21)
气体吸附诱发煤体劣化的试验研究与分析 .....	李清川,王汉鹏,袁亮,等(38)
大倾角工作面飞矸冲击损害及其控制 .....	伍永平,胡博胜,皇甫靖宇,等(55)
锚注扩散及加固规律现场试验研究与应用 .....	王琦,许英东,许硕,等(69)
基于大范围岩层控制技术的大倾角煤层区段煤柱失稳机理研究 .....	伍永平,皇甫靖宇,解盘石,等(84)
大变形巷道螺纹钢锚杆外形优化设计及应用研究 .....	张明,CAO Chen,赵象卓,等(100)
单轴压缩下含瓦斯煤破坏过程能量演化规律 .....	张冰,王汉鹏,袁亮,等(117)
泥质胶结岩体力学特性宏观模拟研究 .....	孙长伦,李桂臣,何锦涛,等(132)
区段煤柱稳定性研究的新探索 .....	闫帅,柏建彪(145)
拉伸荷载下盐岩力学及声发射特征研究 .....	曾寅,刘建锋,邓朝福,等(158)
负压条件下瓦斯渗流实验及抽采模拟研究 .....	李祥春,高佳星,李安金,等(171)
静水压力下开挖卸荷快慢对硐室围岩变形-开裂影响的连续-非连续方法模拟 .....	王学滨,芦伟男,白雪元,等(193)
极软弱地层双层锚固平衡拱结构形成机制研究 .....	孟庆彬,韩立军,梅凤清,等(204)
Deformation and stress analysis of surface subsidence at the Jingerquan Mine .....	DING Kuo,MA Fengshan,ZHAO Haijun,et al(223)
光纤光栅煤矿安全智能监测系统 .....	方新秋,吴刚,梁敏富,等(237)
Repairing technology based on analysis of deformation or failure on main roadways in Shuanglong Coal Mine .....	YUN Dongfeng,WANG Zhen,WU Yongping,et al(248)
Study on the height of fractured zone in overburden at the high-intensity longwall mining panel .....	GUO Wenbing,ZHAO Gaobo,LOU Gaozhong,et al(266)
断层破碎带区域巷道围岩差异性分类及关键控制对策 .....	赵启峰,张农,李桂臣,等(277)
近距离巨厚坚硬岩层破断失稳特征及分区控制 .....	赵通,刘长友(289)
深井软岩下山巷道群非对称破坏机理与控制研究 .....	刘帅,杨科,唐春安(301)

大倾角煤层大采高工作面倾角对煤壁片帮的影响机制 ...	王红伟,伍永平,罗生虎,等(323)
基于 VRP 的采矿过程矿石质量智能优化研究 .....	李小帅,郭连军,徐振洋,等(335)
Assessing longwall shield-strata interaction from a basic understanding of shield characteristics and a physical modeling study .....	SONG Gaofeng,DING Kuo,SUN Shiguo(343)
Strata movement law and support capacity determination of a upward-inclined fully-mechanized top-coal caving panel .....	KONG Dezhong,LIU Yang,ZHENG Shangshang,et al(364)
厚硬岩层直覆大倾角综采顶板失稳机理分析 .....	魏祯,杨科,池小楼,等(375)
长壁充填开采充填步距对覆岩位移的影响分析 .....	贾林刚,高庆丰(382)
近水平厚煤层沿空巷道位置选择及支护技术研究.....	王志强,苏越,苏泽华(393)
沿空留巷可缩性墩柱破坏形态及加固分析 .....	郭东明,凡龙飞,王晓辉,等(406)
优化露天矿山爆堆单元划分方法与出矿品位确定 .....	王雪松,徐振洋,李小帅,等(414)
动载作用下岩石破坏模式与强度特性分析.....	王军(421)

# Detection of floor water inrush risks for deep longwall mining in a Chinese coal mine

HE Dongsheng<sup>1</sup>, ZHANG Yang<sup>2</sup>, WANG Fangtian<sup>2</sup>

(1. Chengjiao Coal Mine, Henan Zhenglong Coal Industry Co. Ltd., Yongcheng 476600, China;

2. School of Mines, State Key Laboratory of Coal Resources and Mine Safety, Key Laboratory of Deep Coal Resource Mining, Ministry of Education of China, China University of Mining and Technology, Xuzhou 221116, China)

**Abstract:** Floor pressurized water inrush is a key problem that threatens safe and efficient production in coal mines, especially in deep longwall coal mining. Depending on the conditions of the aquifer, the hydrogeological conditions become quite complex, leading to a high water pressure environment. As the risk posed by floor pressurized water increases, prevention of water inrush risk in deep coal seams mining becomes crucial. In this study, the hydrogeological conditions of deep coal seams in Chengjiao Coal Mine were analyzed alongside the composition, microstructure, and mineral disintegration of mudstone and sandstone. The two rocks from floor strata were tested in the laboratory to gain important baseline data for a scientific evaluation of the water resistance ability. The seepage resistance strength and permeability coefficient of the rocks at different floor depths were obtained through the in-situ double-hole method detection. A combination method of both fractal dimension of fault complexity and water inrush coefficient was used to evaluate the water inrush risk. As a result, the comprehensive evaluation division of the water inrush risk at Level-II is that the danger decreasing from the eastern area, and then the western area, and last the middle area. A prevention strategy, include advanced warning monitoring, hydrological dynamic monitoring, partial discharge testing, water drainage, pressure reduction, and grouting reinforcement, was applied to enable the safe longwall mining of the deep coal seam with high water inrush risk.

**Keywords:** deep buried coal seam; water inrush risk; water resisting strength; field detection; safe and efficient mining

## 1 Introduction

Mine water damage is the “second killer” threatening mine safety production. From 2000 to 2012, there were 1,069 mine water inrush accidents in China, leading to 4,333 deaths and economic losses of more than 35 billion RMB<sup>[1]</sup>. With the continuous increase in coal mining depth, the threat of mine water hazards has been aggravated, which seriously restricts safe and efficient mining<sup>[2]</sup>. Mine floor water inrush accidents are mainly caused by the original geological structure, with the fault structure being the main precipitating factor<sup>[3, 4]</sup>.

Supported by the Fundamental Research Funds for the Central Universities(2018ZDPY05), the Scholarship Program from China Scholarship Council, and the Priority Academic Program Development of Jiangsu Higher Education Institutions.

Corresponding author: wangfangtian111@163.com.

Research on coal mine water inrush mechanisms and related prevention measures has been popular in China in recent years. Wu et al. systematically classified types of mine water hazards, analyzed the characteristics of coal mine hydrogeology and water disaster problems faced by four coal mine areas, and provided the basis for the classification and prevention of mine water hazards<sup>[5, 6]</sup>. Yin focused on water inrush in mines and divided floor pressurized water inrush into three models: normal floor pressurized water inrush, water inrush from fault fissure zones, and water inrush from collapse columns. Thus, he analyzed the water inrush mechanisms in detail<sup>[7]</sup>. Sun et al. presented a water-resistant key floor strata model, prior to main roof weighting, to explore the relationship between floor water inrush and the main roof weighting<sup>[8]</sup>. Xu divided floor pressurized water inrush into the complete water inrush mode and fault water inrush mode with a water-repellent layer<sup>[9]</sup>. Li et al. utilized fractal theory to conduct a relationship analysis of fault complexity degree and water irruption rate, which was found to increase with the fractal dimension<sup>[10]</sup>. After studying the hydrogeological conditions and type of water inrush passage in the Zhengzhou mining area, Dong categorized mine water inrush into three modes, which are fault-induced mode, fold-induced mode, and mining-fracture-induced mode. He also suggested prevention and mitigation measures based on the applicable water inrush mode<sup>[11]</sup>. Xu et al. proposed three types of trapezoidal broken models considering the top-down varying pattern of the lateral and longitudinal volume expansion coefficients. These models may conduce to understand the caving mechanism of overburden strata and the formation of fracture space, and thence provide guidelines for coal mining under water bodies<sup>[12]</sup>. Wang et al. constructed a secondary fuzzy comprehensive evaluation system to assess the risk of floor water invasion in coal mines. The engineering evaluations were conducted using hydrogeological data of six mining faces<sup>[13]</sup>. Predicting the water inrush potential and taking effective measures before mining activities are essential to enable safe coal mine production<sup>[14]</sup>. However, the prediction of floor pressurized water is closely related to the hydraulic characteristics of floor rock and the distributions of the fault structure.

A deep coal seam (depth over 800 m) at Chengjiao Coal Mine was taken as the research objective. The composition, microstructure, and mineral disintegration of mudstone and sandstone were tested in the laboratory to gain important baseline data for a scientific evaluation of the water resistance ability. The seepage resistance strength and permeability coefficient of the floor rocks were obtained through the in-situ double-hole method detection. To evaluate the floor water inrush risk, a combination of fault complexity fractal dimension and water inrush coefficient was applied. Consider the water inrush risk division at Level-II, a systemic prevention strategy, include advanced warning monitoring, water drainage, pressure reduction, and grouting reinforcement, can be applied to enable the safe and efficient longwall mining of the deep coal seam. The study at Chengjiao Coal Mine attempt to provide some significances for the detection and prevention of floor water inrush risks with similar conditions.

## 2 Hydrogeological background

The Chengjiao Coal Mine is located in Yongcheng City, Henan Province, China. It has a capacity of 5 million t/a, and the main mining of No. 2-2 coal seam is as deep as 1,000 m, the geological columnar section of the floor strata is shown in Fig. 1. The hydrogeological conditions at Level-II (elevation -800 m) are complex: (1) Aquifer development. Coal-bearing formations contain loose rock-like pore-fractured aquifers, Permian sandstone fractures, and the Taiyuan Formation limestone insolvent aquifer; (2) The geostructure water control conditions are complex. Structural networks with unequal scales and different sequence periods not only constitute a direct water-filling channel, but also disturb the stratum structure and reduce the water resisting capacity for the floor rocks, which strengthens the hydraulic links between aquifers to some extent; (3) The complex geological environment of high water pressure, high geostress, high temperature and mining-induced disturbance. The Carboniferous Taiyuan Formation contains a regional aquifer composed of limestone in the floor, which is likely to lead to a water inrush accident.

Till 2017, two water inrush accidents occurred in the Taiyuan formation:

(1) On March 29, 2004, the water inrush occurred in working face LW2205 through a fault structure, the maximum water inflow being 80 m<sup>3</sup>/h. This accident caused the face to withdraw to a distance of 55 m from the stoppage line, resulting a large amount of coal loss.

(2) On June 24, 2008, water inrush occurred during the 1,117 m excavation of the southern area of a rail transport roadway. The initial water volume was 80 m<sup>3</sup>/h, while the maximum water inflow was 300 m<sup>3</sup>/h, gradually stabilizing to 230 m<sup>3</sup>/h. The water inrush was caused by the fault F<sub>N5</sub> along the left-hand roadway. The deep limestone water from the fault plane collapsed into the working face. The increase in mining depth caused a rise in water pressure in the limestone aquifer and lead to a disturbance in the deformation degree of the mining floor. Managing such water hazards in deep coal seam mining is quite difficult. They pose major problems with respect to mine safety and encumber high-efficiency production.

## 3 Laboratory experiment for the floor rocks

Borehole sampling at Level-II (Fig. 1) was conducted to analyze the composition, microstructure and mineral disintegration of mudstone and sandstone from the floor strata. The samples were experimented through the use of D8 Advance type X-Ray Diffraction, Quanta 250 type Scanning Electron Microscope in laboratory to ascertain important baseline data for scientifically evaluating the floor water resisting ability.

### 3.1 Rock mineral composition

As shown in Fig. 2, a comparison of X-ray diffraction results before and after mine water immersion was conducted for mudstone and sandstone samples. The two lithological formations are mainly composed of quartz, and the other minerals are mica and chlorite.

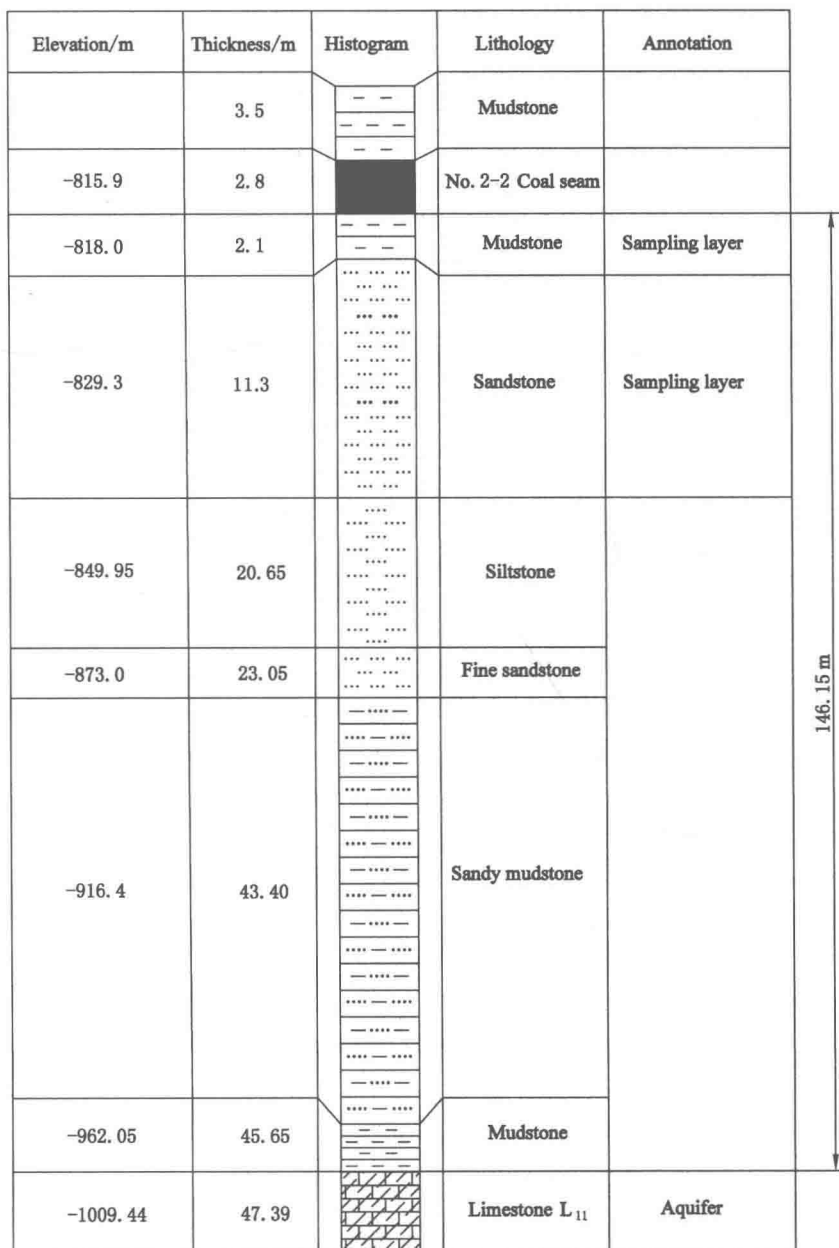


Fig. 1 Geological columnar section of the floor strata

Two sets of X-ray fluorescence tests both reveal that the main components of mudstone and sandstone are silicon and aluminum. The  $\text{SiO}_2$  contents of the mudstone and sandstone are  $\sim 57\%$  and  $\sim 73\%$ , respectively.  $\text{Al}_2\text{O}_3$  being the next most prominent compound, followed by smaller amounts of iron, carbon, potassium, magnesium, sodium and calcium compounds. The high content of siliceous material is the primary reason for relatively high water resisting ability for both mudstone and sandstone. The laboratory

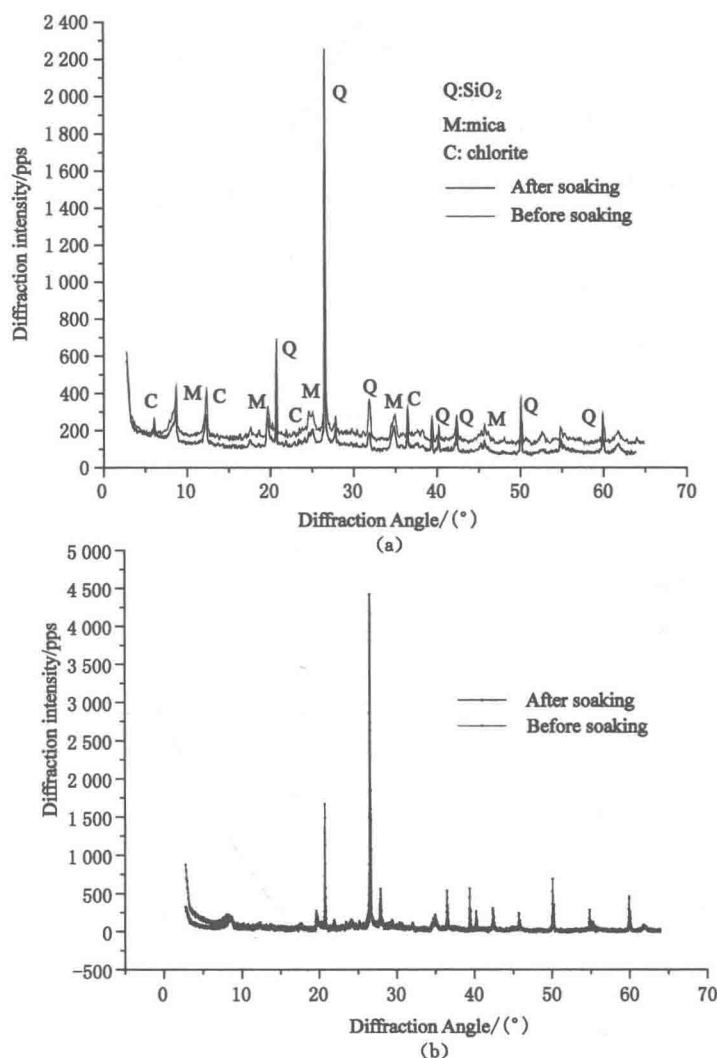


Fig. 2 Comparison of mineral compositions via X-ray diffraction before and after groundwater soaking  
(a) Mudstones; (b) Sandstones

experiment results are shown in Table 1. The comparison of the molecular composition indicated that mudstone and sandstone have the same molecular formula and small change in content before and after soaking, respectively.

Table 1 X-ray fluorescence studies on the composition and content of mudstone and sandstone

Mudstone samples			Sandstone samples		
Molecular formula	Contents before soaking/%	Contents after soaking/%	Molecular formula	Contents before soaking/%	Contents after soaking/%
SiO <sub>2</sub>	57.08	57.24	SiO <sub>2</sub>	73.14	72.64
Al <sub>2</sub> O <sub>3</sub>	20.33	20.28	Al <sub>2</sub> O <sub>3</sub>	17.19	17.72

Continued Table 1

Mudstone samples			Sandstone samples		
Molecular formula	Contents before soaking/ %	Contents after soaking/ %	Molecular formula	Contents before soaking/ %	Contents after soaking/ %
Fe <sub>2</sub> O <sub>3</sub>	8.76	8.79	K <sub>2</sub> O	3.47	3.57
CO <sub>2</sub>	6.33	6.17	Fe <sub>2</sub> O <sub>3</sub>	1.38	1.42
K <sub>2</sub> O	3.56	3.56	CaO	1.32	1.33
MgO	1.83	1.84	CO <sub>2</sub>	1.18	0.96
Na <sub>2</sub> O	0.66	0.65	Na <sub>2</sub> O	1.05	1.05
CaO	0.42	0.43	MgO	0.64	0.67

3.2 Microstructure analysis

Changes in the contents of the mineral components will inevitably lead to changes in the microstructure. As per Fig. 3 (a) and (b), the mudstone is compact before groundwater soaking, only part of the bedding has developed micro-fractures, and the density of micro-fissures is low. After groundwater soaking, the microstructure of the mudstone is loose, showing more developed micro-fractures, which is the reason that easy to fracture along the joint surface in the disintegration test. Fig. 3 (c) and (d) show a micro-fissure magnified by 1,200× before groundwater soaking, and the characteristics of the sandstone after groundwater soaking are similar to those of mudstone.

The comparison indicates that (1)ground water soaking increases the micro-fissures of the rock’s surface, (2) after soaking, the rock tends to break easily, (3) surface micro-fissures increase in number as well as size, (4) the rock around the fissures dissolves, (5) and the microstructure angularity of the soaked rock surface is pronounced due to the heterogeneous dissolution of the rock.

3.3 Disintegration tests of the floor rocks

Table 2 shows the disintegration test classifications according to Gamble’s disintegration durability classification.

Table 2 Classification reference table for disintegration durability as per Gamble<sup>[15]</sup>

Group	Percentage left after one 10-min rotation/ %	Percentage left after two 10-min rotations/ %
Extremely high durability	>99	>98
High durability	98~99	95~98
Medium high durability	95~98	85~95
Moderate durability	85~95	60~85
Low durability	60~85	30~60
Extremely low durability	<60	<30

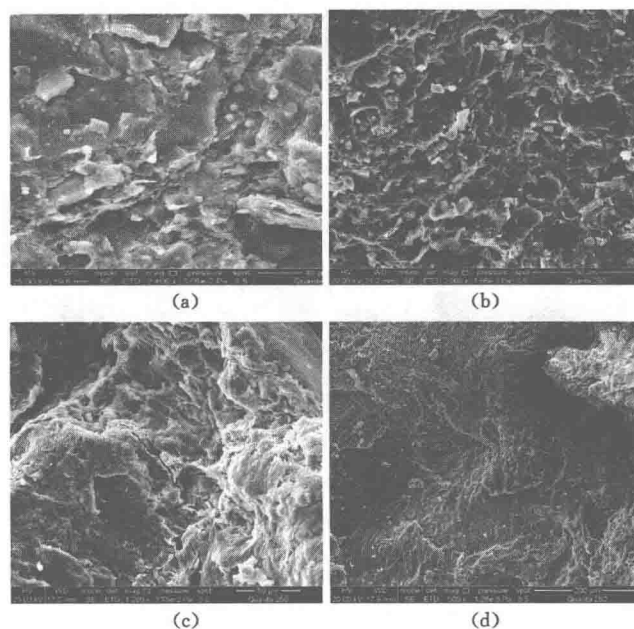


Fig. 3 Scanning electron microscopy contrast images of mudstone

and sandstone before and after ground water soaking

(a) Before soaking in mudstone; (b) After soaking in mudstone;

(c) Before soaking in sandstone (magnify 1200 times);

(d) After soaking in sandstone

The SCL-1 disintegration resistance tester (manufactured by Hangzhou Sansi Instrument Co. Ltd., China) was used for this test. The disintegration apparatus and images of sample baking are shown in Fig. 4.

(1) Mudstone: The mudstone specimens were square-shaped. The experimental phenomena related to the disintegration and the test results are shown in Table 3 and Table 4, respectively.

Table 3

Disintegration phenomena

2 <sup>nd</sup> drying	3 <sup>rd</sup> drying	4 <sup>th</sup> drying	5 <sup>th</sup> drying	6 <sup>th</sup> drying
No. 3 split into two along the cleavage plane and No. 1 cracked	No. 3 retains two pieces, and No. 1 split into two large parts along the cleavage surface and several small pieces were also formed	No changes were noted in Nos. 3 and 1	One of the two pieces of No. 3 split along the bedding plane again, and three pieces in all. No other changes were noted	A large piece of the cracked No. 1 split into two small pieces along the cleavage surface, and several small pieces were also formed

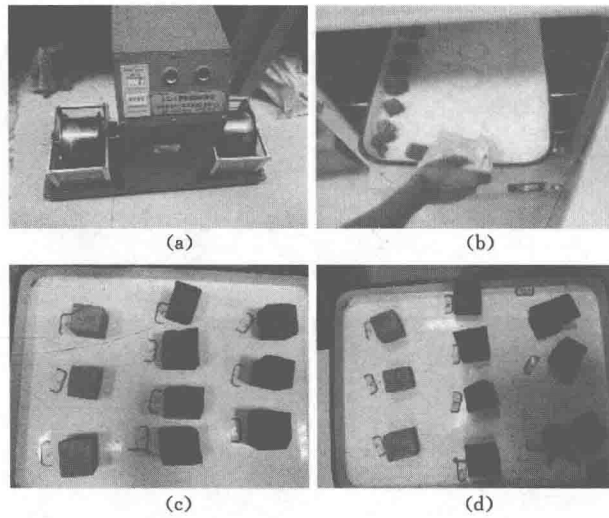


Fig. 4 Instrument and images of sample baking for the sample disintegration test  
(a) Disintegration tester; (b) Sample baking; (c) Before disintegration; (d) After disintegration

**Table 4** Experimental results of mudstone disintegration

No.	Sample quantity/g						Id/%
	Before the experiment A	After the 1 <sup>st</sup> cycle B	After the 2 <sup>nd</sup> cycle C	After the 3 <sup>rd</sup> cycle D	After the 4 <sup>th</sup> cycle E	After the 5 <sup>th</sup> cycle F	F/A×100%
1	129.4	129.4	129.2	129.0	128.7	128.5	99.3
2	106.4	106.4	106.3	105.9	105.7	105.6	99.2
3	100.0	100.0	99.8	99.6	99.5	99.4	99.4

Note: Id is the disintegration resistance index, F is the quality after the fifth cycle, and A refers to the quality before the experiment.  $Id(\%) = F/A \times 100\%$ .

Mudstone disintegration is due to the dissolution of soluble clay minerals when interacting with water, which results in loss of adhesion and weakens the structural connection within the mudstone. Thus, the material loses strength. The mudstone presents in the deep floor, which has not been subjected to natural weathering and has undergone a relatively high degree of consolidation. Its internal structural connection strength is high and the macroscopic appearance confirms disintegration. According to Table 4, the disintegration resistance index of the collected mudstone samples ranges from 99.2% to 99.4%, indicating that the rock has extremely high durability.

(2) Sandstone: The disintegration test results for the sandstone are shown in Table 5. The disintegration resistance index lies between 99.4% and 99.9%, confirming that the rock has extremely high durability.

Table 5 Experimental results of sandstone disintegration

No.	Sample quantity/g						Id (%) F/A×100%
	Before the experiment A	After the 1 <sup>st</sup> cycle B	After the 2 <sup>nd</sup> cycle C	After the 3 <sup>rd</sup> cycle D	After the 4 <sup>th</sup> cycle E	After the 5 <sup>th</sup> cycle F	
A1	93.6	93.5	93.5	93.2	93.1	93.1	99.7
A2	70.2	70.0	70.0	69.9	69.8	69.8	99.4
A3	86.6	86.5	86.3	86.2	86.2	86.2	99.5
B1	112.4	112.4	112.5	112.4	112.4	112.3	99.9
B2	119.0	119.0	118.9	118.9	118.8	118.7	99.7
B3	112.9	112.9	112.8	112.8	112.8	112.6	99.7

Through the microstructure, comparison and disintegration laboratory experiment, and also the analysis of different floor rock samples before and after soaking tests, which indicate that the microstructure and composition have little change before and after ground water soaking, and the main floor rocks at Level-II have good water stability characteristics.

4 Field detection of the floor water resisting ability

Longwall mining in the normal sedimentary area is very safe at Chengjiao Coal Mine, but the situation is different in some structurally affected areas: (1) The mudstone in the floor has a good water resisting property, but its structural integrity will be damaged inordinately due to the thickness decreases and fault structure changes, therefore results in a sharp decrease of the floor water resisting strength; (2) The effects of longwall mining easily magnify at some fault structural zones and can activate fissures, thus greatly increasing the danger of underground pressured water inrush risks. Thus, the hidden dangers of longwall mining under floor pressured water mainly depend on the fault structural development. Therefore, a floor water resisting ability test is required in the field.

4.1 Main principles and equipment

This study uses the double-hole pressurization test technique. Two boreholes were arranged in the roadway, one for water injection and the other for hydraulic test (Fig. 5). By testing the water pressure conditions for low-resistance seepage in the rock formation, the permeability of the floor rock, permeation, and failure strength of a unit thickness are obtained, which provide a quantitative basis for the evaluation of floor water resisting ability. During the process of water injection, parameters such as water injection pressure, water injection flow rate, and infiltration water pressure value can be measured to obtain the water resisting strength and permeability coefficient of the rock formation at different floor depths.